Special Section: Contaminants in the Vadose Zone

Zhiming Lu*
Edward M. Kwicklis

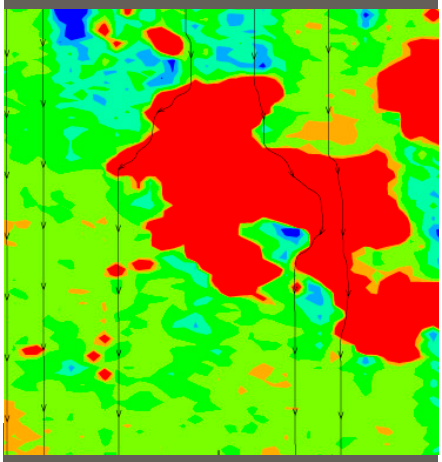

A numerical procedure for estimating effective block parameters (conductivity, van Genuchten parameters) of unsaturated porous media from fundamental fracture properties such as spacing and aperture is developed. These effective parameters are independent of pressure head or saturation and can be assigned to grid nodes in field-scale simulations.

Z. Lu and E.M. Kwicklis, Computational Earth Sciences Group (EES-16), MS T003, Los Alamos National Labora-tory, Los Alamos, NM 87545, USA. *Corresponding author (zhiming@lanl.gov).

Vadose Zone J.
doi:10.2136/vzj2011.0164
Received 15 Nov. 2011.

© Soil Science Society of America
5585 Guilford Rd., Madison, WI 53711 USA.
All rights reserved. No part of this periodical may be reproduced or transmitted in any form or by any means, electronic or mechanical, including photocopying, recording, or any information storage and retrieval system, without permission in writing from the publisher.

Numerical Evaluation of Effective Unsaturated Hydraulic Properties of Fractured Rocks using a Stochastic Continuum Approach

This study builds on past studies that have investigated the effective properties of unsaturated porous media and merges stochastic continuum concepts to develop a numerical procedure for estimating the effective flow parameters that are independent of pressure head or saturation. The procedure involves the development of a numerical permeameter based on randomly generated, spatially correlated fields of fundamental fracture properties such as spacing and aperture. Local values of hydraulic conductivity, and the van Genuchten fitting parameters α and n in this random field are computed from local values of mechanical aperture and spacing based on the cubic law and relationships established from pore-scale fracture simulations. By considering multiple realizations of these spatially correlated fields and by running the numerical permeameter over a range of effective saturations and flow rates, outputs are generated that can be fit with the standard van Genuchten model to estimate block effective values of saturated hydraulic conductivity and the van Genuchten unsaturated hydraulic parameters of a fracture continuum at the field scale. These parameters can then be incorporated to conventional numerical simulators originally developed for porous media. The study shows that reasonable approximations to the results obtained through computationally demanding stochastic simulations can be developed based on estimates of the mean fracture spacing and aperture. Although the example application assumes the presence of an impermeable rock matrix, the hydraulic properties estimated for the fracture continuum with this methodology can be combined with those measured or similarly estimated for a matrix continuum in dual-permeability continuum models.

It is well known that geologic formations, whether fractured or not, are heterogeneous at various length scales. One approach to modeling flow in such heterogeneous formations is to incorporate the heterogeneity directly into the numerical model by designing the grid based on the distribution of the heterogeneities. However, even with this approach, one is confronted with the challenge of how to consider processes and heterogeneities at the subgrid scale. An alternative approach is to represent a heterogeneous medium by an equivalent homogeneous medium with upscaled (effective) flow properties and thereby predict the mean flow behavior at the field scale. Quite often, one may need to assign medium properties to numerical grid blocks that are much larger than the support scale at which medium properties are measured at some locations. The question is how to represent a block of a heterogeneous medium by equivalent homogeneous one and then estimate effective block flow properties that represent this equivalent homogeneous medium.

Numerous studies have investigated the effective properties for partially saturated porous media, including theoretical work (Yeh et al., 1985; Mantoglou and Gelhar, 1987; Zhu and Sun, 2009, among others), numerical simulations (Wildenschild and Jensen, 1999a; Khaleel et al., 2002), and experimental studies (Wildenschild and Jensen, 1999b). Most of these studies focus on estimating effective hydraulic conductivity under different tension or pressure. One of the important findings was that the effective unsaturated conductivity depends on the pressure head (Yeh et al., 1985; Khaleel et al., 2002). However, difficulty arises when applying the pressure-dependent effective unsaturated conductivity to the field-scale simulations, because one does not know in advance the pressure head at all grid nodes in the flow domain, unless the flow field is solved first, which defeats the purpose of the upscaling. This suggests the need for a methodology that is capable of estimating effective parameters that are independent of pressure head, while these parameters can represent the unsaturated conductivity for a broad range of pressure or saturation.

We propose a numerical upscaling approach to derive effective soil parameter values that are independent of pressure head or saturation, which means that such effective parameter values can be assigned to numerical grids in simulating flow and transport in unsaturated rocks. We first run a number of flow simulations under a gravity-dominated condition, using realizations of saturated conductivity K_s, the air-entry parameter α, and the pore-size distribution parameter n. The size of the simulation domain can be chosen close to the block size typically used in the field-scale models. For some recent unsaturated-zone site models (e.g., Wu et al., 1999), grid cell dimensions can be hundreds of meters in the horizontal directions and many tens of meters in the vertical direction. The gravity-dominated condition is achieved by maintaining the same saturation at the top and bottom of the simulation domain. The effective unsaturated conductivity for each simulation is determined from the steady state flux at the bottom of the domain. The relationship between all pairs of the effective unsaturated conductivity and the mean pressure head (or mean saturation) is then fitted using the van Genuchten model to obtain the effective values $K_{s,\mathrm{eff}}$, α_{eff}, and n_{eff}. These effective parameters are valid for a range of pressure head (or saturation), which allows us to use these effective values in field-scale modeling.

The upscaling procedure is applied to unsaturated fractured rocks. A discrete fracture representation of a highly fractured groundwater aquifer is inappropriate as a modeling approach because the location of all fractures can never be explicitly specified. In this study, hydrologic properties of fractured rocks are represented with a stochastic continuum model. The concept of continuum model for fractured rocks can be traced back to Bibby (1981) on the dual porosity model. Numerous studies have been conducted since then (Berkowitz et al., 1988; Neuman, 1987; Tsang et al., 1996; Finsterle, 2000 among others). The basic idea behind this approach is that the fracture network is approximated at the local measurement scale (sometimes referred to as the "support" scale) as a continuum with spatially variable hydraulic and transport properties. The properties of the continuum at the local measurement scale vary in space and are correlated spatially in a way that reflects the connectivity and orientation of the fracture network. For instance, using kriging techniques, the correlation in the vertical direction could be made much smaller than the correlation scale in the horizontal direction if the fractures are strata bound, or conversely, the vertical correlation lengths could be made much larger than the horizontal correlation lengths to mimic the presence of steeply dipping fault zones. In our application of the stochastic continuum concept to unsaturated, fractured rock, the measurements at the support scale are mechanical fracture aperture and fracture spacing. These randomly generated stochastic fields are then used with a variant of the well-known cubic law to generate spatially correlated fields of hydraulic conduc-tivity and fracture porosity. For unsaturated hydrologic properties, the stochastic continuum representation uses relationships between fracture's mechanical aperture and unsaturated hydraulic properties developed for single fractures (Kwicklis and Healy, 1993; Kwicklis et al., 1998). As discussed below, the statistics of fracture aperture and spacing were estimated from tuffs in the vicinity of the Nevada Test Site.

To demonstrate the applicability of the upscaling methodology, flow simulations are performed in a larger, field-scale domain with different scenarios of K_s, α, and n fields. Three types of flow simulations were conducted: one simulation with mean parameter values, one simulation with effective parameter values derived from this proposed approach, and Monte Carlo simulations with a large number of realizations of K_s, α, and n fields. Results from Monte Carlo simulations are considered as "true" solutions to the unsaturated flow problem and the results from other two types of simulations are compared to Monte Carlo results.

Conceptual Model

We consider unsaturated steady state flow in three-dimensional, bounded, randomly heterogeneous media governed by the Richards equation,

$$\nabla\cdot\left\{K(\psi,\mathbf{x})\nabla\left[\psi(\mathbf{x})+x_3\right]\right\}=0 \qquad [1]$$

where ψ is the pressure head, K is the unsaturated hydraulic conductivity, and $\mathbf{x} = (x_1, x_2, x_3)^{\mathrm{T}}$ is the vector of Cartesian coordinates. The elevation x_3 is directed vertically upward. This equation is nonlinear because the unsaturated hydraulic conductivity depends on the pressure head. To solve this nonlinear equation, one has to specify the constitutive relationship between the pressure head and unsaturated hydraulic conductivity. The van Genuchten–Mualem model (van Genuchten, 1980; Mualem, 1976) is adopted in this study:

$$K(\mathbf{x})=K_s(\mathbf{x})\sqrt{S(\mathbf{x})}\left\{1-\left[-\alpha(\mathbf{x})\psi(\mathbf{x})\right]^{n(\mathbf{x})}\right\}^2 \qquad [2]$$

$$S(\mathbf{x})=\left\{1+\left[-\alpha(\mathbf{x})\psi(\mathbf{x})\right]^{n(\mathbf{x})}\right\}^{-m(\mathbf{x})} \qquad [3]$$

where K_s is the saturated hydraulic conductivity, S is the saturation defined as $S = (\theta - \theta_r)/(\theta_s - \theta_r)$, θ is the water content, θ_s is the saturated water content, θ_r is the residual water content, α is related to the inverse of the air-entry pressure, n is related to the pore size distribution, and $m = 1 - 1/n$. To solve Eq. [1] numerically with the constitutive model (Eq. [2–3]), one needs to specify values of these parameters at all grid nodes. Since the spatial distributions of these parameters are unknown, one has to treat these parameters as stochastic quantities and therefore Eq. [1] becomes stochastic.

Discrete fracture network and stochastic continuum are two commonly used approaches in simulating flow and transport in fractured rocks. In this study, the stochastic continuum approach

is used and the aperture and fracture spacing are considered as continuous random fields. We assume that α and n are related to the mean physical aperture b_m (in micrometers) by the following empirical relationships (Kwicklis et al., 1998):

$$\alpha = 0.1 b_m + 1.35 \times 10^{-4} b_m^2 \quad [4]$$

$$n = 2.7662 + 18.608 / b_m \quad [5]$$

and the permeability of a single fracture is given as (Kwicklis et al., 1998):

$$k_f = 10^{-12} b_h^3 / 12 b_m \quad [6]$$

where $b_h = 0.5575 b_m$ is the hydraulic aperture. The simulated hydraulic aperture b_h is calculated as approximately half the mean physical aperture b_m because of tortuosity and flow constrictions in the two-dimensional flow field caused by small aperture segments within the variable aperture fractures. This is in agreement with laboratory measurements of hydraulic and mean physical apertures, which indicate that b_h is approximately 0.3 to 0.5 b_m (Zheng et al., 2008). Laboratory data and theoretical arguments also indicate b_m provides a close approximation of the mass balance aperture to be used for transport calculations (Zheng et al., 2008; Tsang, 1992).

The permeability of fracture rocks can be derived from a variation of the well-known cubic law, which accounts for differences in mechanical and hydraulic aperture:

$$k = k_f \varphi_f = k_f (b_m / s) = 1.44 \times 10^{-20} b_m^3 / s \quad [7]$$

where $\varphi_f = b_m/s$ is the fracture porosity, and s is the fracture spacing [m], which is the inverse of fracture density. Equivalently, saturated hydraulic conductivity [m/s] can be converted from permeability [m^2] by $K_s = 9.756 \times 10^6 k$.

The statistics of parameters α, n, and k may be determined from Eq. [4–7] using those of b_m and s. By assuming that the aperture and spacing is uncorrelated, it is easy to show that permeability k follows a log normal distribution with

$$\langle \ln k \rangle = -45.687 + 3 \langle \ln b_m \rangle - \langle \ln s \rangle \quad [8]$$

and

$$\sigma_{\ln k}^2 = 9 \sigma_{\ln b_m}^2 + \sigma_{\ln s}^2 \quad [9]$$

Since b_m has a log normal distribution (see next section), the second term in the right side of Eq. [5], denoted as y = 18.608/b_m, also has a log normal distribution with $y \sim N(2.92 - \langle \ln b_m \rangle, \sigma_{\ln b_m}^2)$, and n has a shifted log-normal distribution with mean $\langle n \rangle = 2.766 + \langle y \rangle$ and variance σ_y^2, where $\langle y \rangle$ and σ_y^2 are related to the statistics of b_m:

$$\langle y \rangle = 18.608 e^{-\langle \ln b_m \rangle + \sigma_{\ln b_m}^2 / 2} \quad [10]$$

$$\sigma_y^2 = \langle y \rangle^2 \left(e^{\sigma_{\ln b_m}^2} - 1 \right) \quad [11]$$

It is more complicated to derive the distribution for α. Denoting $\alpha = \alpha_1 b_m + \alpha_2 b_m^2$, from the definition of the cumulative distribution function, one has

$$F_\alpha(x) = P(\alpha \le x) = P(\alpha_1 b_m + \alpha_2 b_m^2 \le x) = P(r_1 < b_m \le r_2) = F_{b_m}(r_2) - F_{b_m}(r_1) \quad [12]$$

where r_1 and r_2 are the roots of the quadratic equation $\alpha_1 b_m + \alpha_2 b_m^2 = x$, and

$$F_{b_m}(z) = \Phi\left(\left[\ln z - \langle \ln b_m \rangle \right] / \sigma_{\ln b_m} \right) \quad [13]$$

where Φ is the cumulative distribution function of the standard normal distribution. One can use Eq. [8–13] to evaluate the mean and variance of k, α, and n. In our simulations, however, instead of generating these parameter values from their distributions, they are converted from realizations of b_m and s using Eq. [4–7].

Statistics of Fracture Parameters

To obtain unsaturated hydraulic parameters (α, n, and k or K_s) using Eq. [4–7] and solve flow equations, one needs to have fracture aperture and spacing at each grid node in the simulation domain. Because of incomplete knowledge of two fracture parameters, one has to rely on stochastic generation of these parameter sets using statistics of fracture aperture and spacing, which in this example are inferred from field measurements.

We took a fracture spacing dataset from sparsely fractured nonwelded tuffs from the Nevada Test Site (Prothro, 2008). This dataset includes data from four boreholes: UE-7f, UE-7az, UE-7ba, and UE-7bc. The fractures encountered in these boreholes have been measured from cores, which allows us to accurately calculate spacing between adjacent fractures. The sample distribution of fracture spacing from all 498 samples was first tested using three statistical tests (Kolmogorov-Smirnov, Anderson-Darling, and Chi-Squared test). For a significance level of 0.05, no test rejected the hypothesis that fracture spacing follows a log-normal

distribution. The mean and variance of log fracture spacing were calculated as $\langle \ln s \rangle = 0.008$ and $\sigma^2_{\ln s} = 2.86$, respectively. The correlation scale in the vertical direction was estimated from variograms. All 498 samples from four boreholes were considered as four realizations of fracture spacing and the variogram computed using these samples was well fitted by an exponential type variogram model $\gamma(h) = C_0 + C^*(1 - e^{-h/a})$ with a nugget effect $C_0 = 1.86$, a sill $C = 2.86$, and a range $a = 33$ m, as showed in Fig. 1a. The nugget effect usually represents measurement errors and the influence of variability at scales smaller than the measurement scale. In our case, since the fracture locations in boreholes were accurately measured, the high nugget may be ascribed to irreducible subgrid variability. Therefore, it has been included in our simulations.

Because this data set does not include aperture measurements, we used a second dataset comprised of in situ air permeability measurements made in unsaturated fractured rock at Yucca Maintain (LeCain, 1997). This dataset are from four boreholes: NRG-6, NRG-7a, UZ-16, and SD-12, from which the aperture was obtained indirectly. This dataset include a number of parameters measured at different depths, two of which are relevant to this study: fracture density and permeability. The number of natural fractures per 10-ft interval at the corresponding depth of each air permeability test was taken from well logs (LeCain, 1997). The averaged fracture spacing was then computed from the length of intervals divided by the number of fractures. The average aperture value for each interval was then determined from the permeability and fracture spacing using Eq. [7]). The sample distribution of aperture values for all 195 injection tests was also tested using the aforementioned statistical tests. For a significance level of 0.05, no test rejected the hypothesis that the aperture follows a log-normal distribution. The mean and variance of the log mechanical aperture (in μm) are $\langle \ln b_m \rangle = 5.534$, and $\sigma^2_{\ln b_m} = 0.38$, respectively. The variogram of log aperture is fitted by an exponential model $\gamma(h) = 0.14 + 0.24(1 - e^{-h/15})$.

Although in this example the fracture spacing and aperture distributions have been developed from different areas and rock types, application of the methodology to particular field sites would preferably involve measurements of both aperture and spacing from the site itself. However, it is interesting to note that detailed flow logs in some parts of the NTS indicate little differences in the permeability of fractures (and presumably fracture apertures) when fractures are encountered in different formations; the main differences in formation behavior are related to the proportion of the formation that have productive fractures.

Permeability and spacing data are obtained from too few boreholes to allow horizontal correlation lengths to be estimated. For illustrating the methodology, it will be assumed that the covariance functions of both fracture spacing and aperture fields are isotropic, i.e., the same correlation lengths in horizontal and vertical directions. However, as mentioned earlier, different correlation lengths for the horizontal direction could have been chosen to represent the presence of strata-bound fractures or steeply dipping fracture or fault zones.

The possible correlation between fracture spacing and fracture aperture may have a significant impact on the effective parameters. However, there is no reliable data available for determining the correlation between these two variables, and therefore they are modeled as independent random fields in this study.

Figure 2 shows one set of realizations of fracture spacing and aperture with their statistics given above, using the random field generator described in Zhang and Lu (2004). The corresponding realization of k permeability, van Genuchten parameters α and n, converted spacing and aperture fields using Eq. [4–7], are illustrated in Fig. 3. As a reference, the statistics of n and k are deter-mined from Eq. [8–10]: $\langle \ln k \rangle = 29.09$(which is equivalent to a geometric mean $k_G = 2.32 \times 10^{-13}$ m^2, or $K_{s,G} = 0.196$ m d^{-1}),

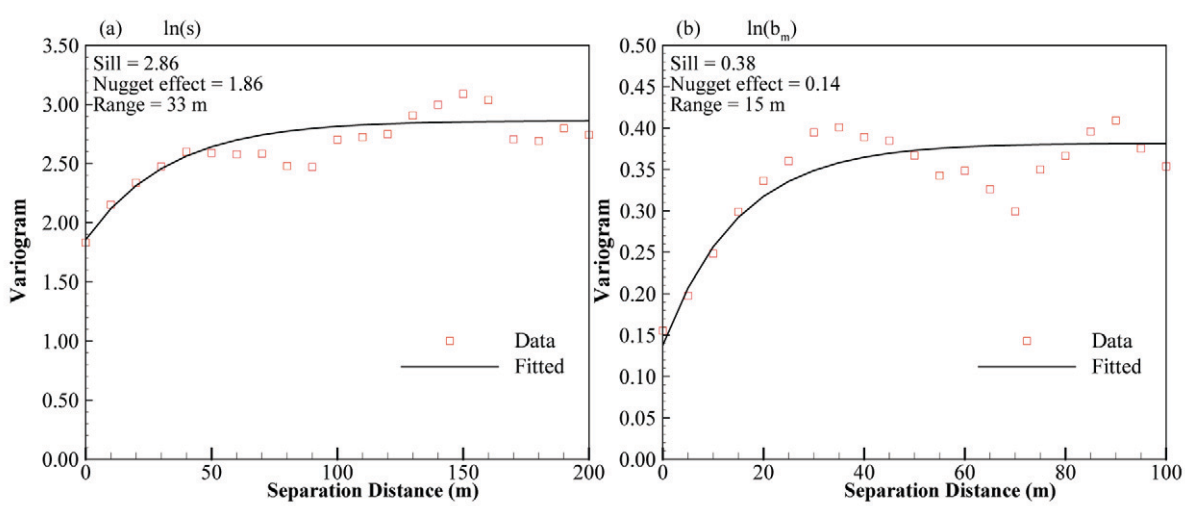

Fig. 1. Variograms computed from field data for (a) log fracture spacing, and (b) log fracture aperture.

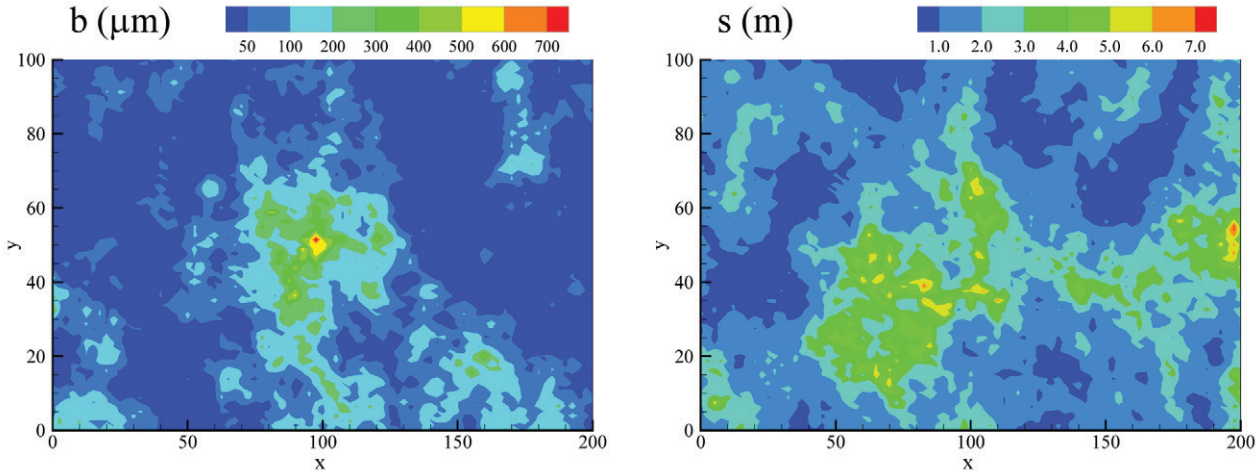

Fig. 2. A set of realizations of aperture and fracture spacing.

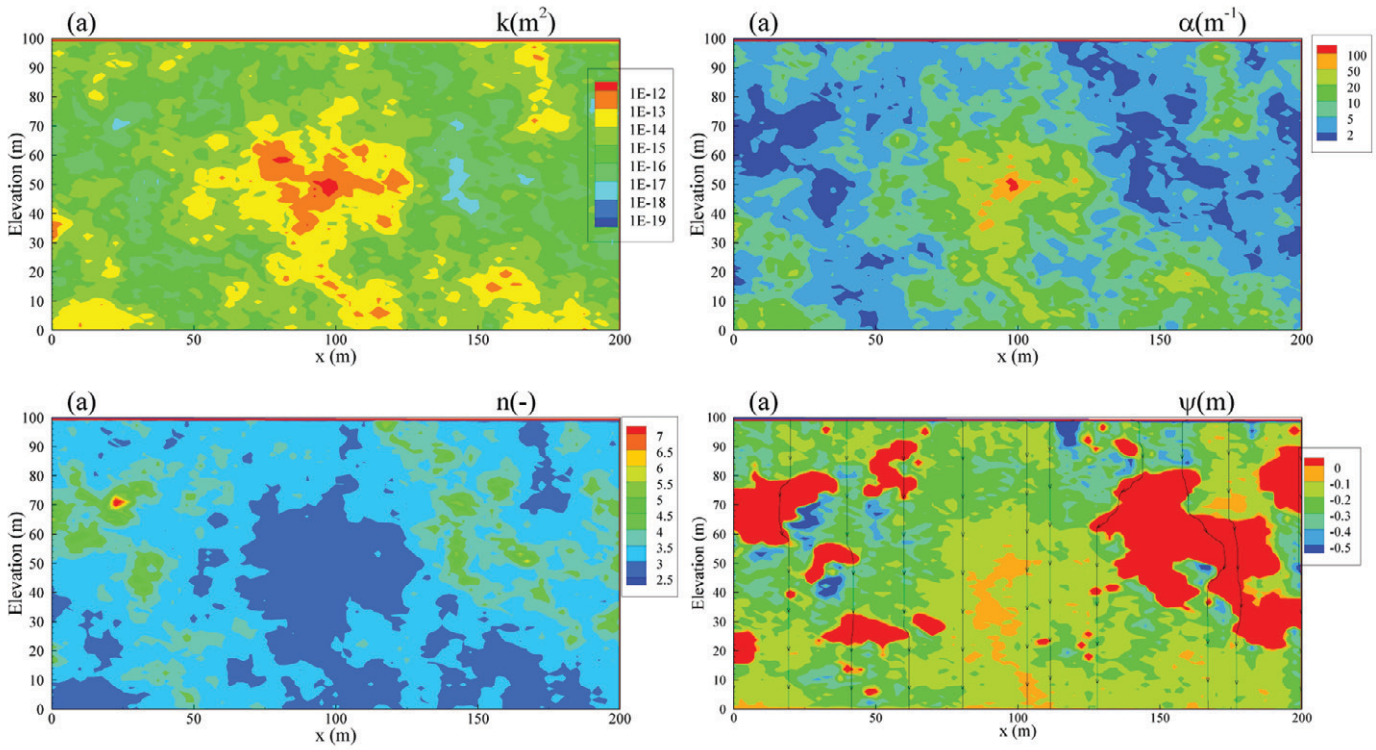

Fig. 3. Realizations of K, α, and n converted from realizations of aperture and spacing shown in Fig. 2, and pressure head field solved from this set of realizations.

$\sigma^2_{\ln k} = 6.29$, $\langle n \rangle = 2.855$, and $\sigma^2_n = 3.6\times10^{-3}$. It is worth to note that the variability of log permeability (which is the same as the variability of log saturated conductivity) is very high. The pressure head field solved from this set of realizations is also shown in the figure for the case with infiltration of 25 mm yr^{-1} at the upper boundary and water table at the lower boundary.

Upscaling Methodology

The goal of this study is to derive pressure-independent effective values of K_s, α, and n for unsaturated fractured rock that can be applied at scales of many tens of meters yet incorporate the effect of subgrid scale heterogeneity. For this purpose, we considered a vertical rectangular domain of size 200 m × 100 m, uniformly discretized into a 160 × 80 numerical grid with $\Delta x = \Delta y = 1.25$ m. The grid size in each axis direction was chosen to be less than

one-fifth of the correlation length so that variations in aperture and spacing could be well captured in the model.

A number of realizations of the log aperture and log spacing fields were generated based on the statistics of aperture and fracture spacing given above, using the random field generator described in Zhang and Lu (2004). These realizations of spacing and aperture were then converted to realizations of k (or K_s), α, and n using Eq. [4–7].

To allow water to enter and exit the fractured rock domain naturally according to permeability variations in the rock, a highly permeable zone that corresponds to permeable sand or vitric tuff was placed at both the top and bottom of the domain. This high permeability layer served as a manifold that would allow water to enter and exit the fractured rock portion of the flow domain without an excess build-up in pressure. The gravity-dominated regime (in the mean) was achieved in the simulation by specifying the same saturation value at both the top and bottom layers and running the model to steady state. This process was repeated at different saturation values to span a range of moisture conditions.

The equation for unsaturated flow was solved using Finite-Element Heat- and Mass-Transfer code (FEHM) developed by Zyvoloski et al. (1997). Since it is computational demanding to solve unsaturated flow in heterogeneous K_s, α, and n fields under the gravity-dominated condition, especially at low saturation levels, we only solved the first 20 sets of realizations. For each set of realizations of K_s, α, and n, a number of steady state simulations were conducted with different saturation values specified at the top and bottom boundaries.

For each simulation, the steady state flux leaving the flow domain from the lower boundary was used to calculate the effective unsaturated hydraulic conductivity corresponding to this realization of random fields of K_s, α, and n at the mean pressure head and saturation within the fractured portion of the flow domain. Because of heterogeneity, both the simulated pressure head and saturation vary spatially, although the mean head and mean saturation are more-or-less constant in the domain. The mean capillary pressure and saturation were computed by averaging the pressure or saturation over the flow domain, excluding their values in the top and bottom layers.

The last step is to fit the numerically derived pairs of the effective unsaturated hydraulic conductivity and mean pressure head (or mean saturation) using the van Genuchten–Mualem model. The values of K_s, α, and n that best fit the data pairs are defined as "effective" parameters $K_{s,eff}$, α_{eff}, and n_{eff}.

The upscaling procedure described above involves a number of critical components: approximating the random parameter fields with a finite number of realizations, the accuracy of numerical solver under very dry conditions, and appropriateness of the curve-fitting algorithms. Before applying the upscaling methodology to random fields of K_s, α, and n, we conducted a test case in which all three parameters are constants $K_s = 0.196$ m d^{-1}, $\alpha = 33.96$ m^{-1}, and $n = 2.84$, which were computed from the mean spacing and mean aperture. Following the above procedure, i.e., running flow simulations under different saturation, computing effective unsaturated conductivity and mean pressure head, and curve-fitting the data pairs using the van Genuchten model, we estimated the "effective" parameter values $K_{s,eff} = 0.199$ m d^{-1}, $\alpha_{eff} = 33.75$ m^{-1}, and $n_{eff} = 2.85$. As expected, these effective values are nearly identical to their original values, indicating that the upscaling procedure is reasonable.

For the generated random fields, the effective unsaturated hydraulic conductivity is plotted as a function of the mean pressure head or mean saturation in Fig. 4a and 4b. Each square symbol in the figures represents the mean pressure head or saturation and their corresponding effective unsaturated conductivity from one flow

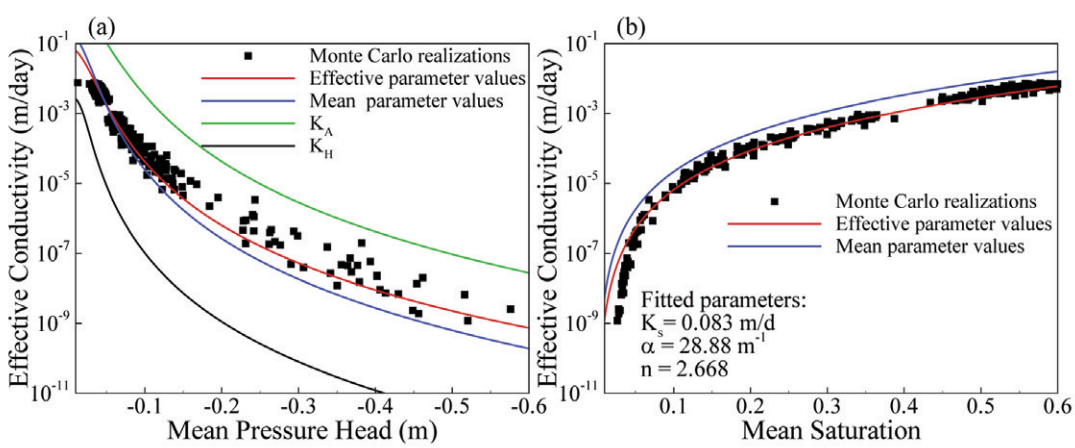

Fig. 4. Comparison of the effective unsaturated conductivity as a function of (a) mean pressure head and (b) mean saturation, using effective parameter values (red curves) and mean parameter values (blue curves) against results from Monte Carlo simulations (dots).

simulation. These data points were then fitted using the van Genuchten–Mualem model, and the corresponding K_s, α, and n in this model were defined as "effective" parameters $K_{s,eff}$, α_{eff}, and n_{eff}. The red curve in the figures is the fitted van Genuchten-Mualem model with parameters $K_{s,eff} = 0.083$ m d–1 (or $k_{eff} = 9.85 \times 10^{-14}$ m^2), $\alpha_{eff} = 28.88$ m^{-1}, and $n_{eff} = 2.668$. This set of effective parameters can be used to represent the unsaturated hydraulic conductivity for a wide range of moisture contents.

For the purpose of comparison, the relationship between the unsaturated hydraulic conductivity and mean pressure head or saturation using mean values $K_s = 0.196$ m d^{-1}, $\alpha_{eff} = 33.96$ m^{-1}, and $n = 2.84$ is also plotted in the figures (blue curves). These mean parameter values are computed from the mean log aperture and mean log spacing using Eq. [4–7]. The figures show that the curves created using the fitted effective parameter values are better than those calculated from the mean parameter values, although the latter also provides a reasonably good approximation to Monte Carlo results at a fraction of computational cost.

The effective conductivity from the direct averaging method (Khaleel et al., 2002) is also compared in Fig. 4a, where K_H and K_A stand for harmonic and arithmetic averaging, respectively. These two values for each pressure head represent two bounding cases and our model simulation results (squares) are bounded by these values.

The effective hydraulic conductivity is plotted against the average saturation of the flow do-main in Fig. 4b. Also compared in the plot are two unsaturated conductivity curves computed from the van Genuchten–Mualem model using the mean parameters and the fitted effective parameters, respectively. It is noted that the curve based on the fitted effective parameters can more accurately fit Monte Carlo results, although the curve based on the mean parameter values can also fit them reasonably well.

The effective parameter values described above are derived for a particular domain size. To investigate the possible effect of the selected domain size on upscaled parameters, the same procedure was repeated using a small domain size of 50 m × 50 m. The grid size for this case was 1 m × 1 m. The results are illustrated in Fig. 5, which indicates that the general trend of dependence of the effective unsaturated conductivity on the mean pressure head is almost the same for both domains, although the variation (spreading) of the effective unsaturated conductivity computed from Monte Carlo flow simulations increases as the size of the domain decreases. The fitted effective parameters for the 50-m × 50-m domain are $K_{s,eff} = 0.095$ m d^{-1} (or $k_{eff} = 1.12\times10^{-13}$ m^2), $\alpha_{eff} = 28.42$ m^{-1}, and $n_{eff} = 2.60$. The similarity of the effective parameter values obtained using two domain sizes suggests that sufficient spatial averaging was achieved at the 200 m × 100 m scale to estimate effective hydraulic properties and that domains larger than those considered here would provide similar results. There is more

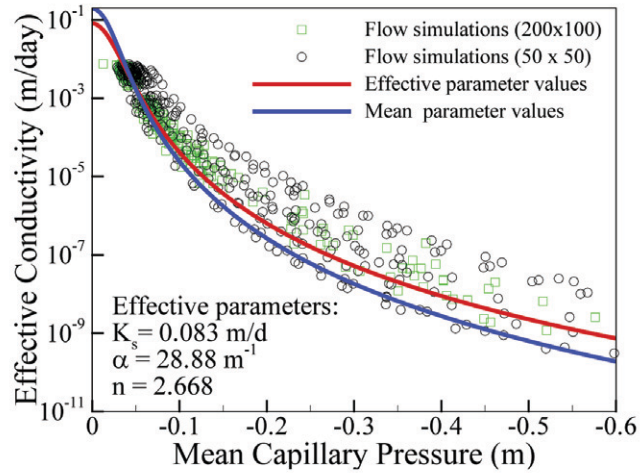

Fig. 5. Comparison of the fitted effective unsaturated conductivity as a function of mean pressure head using effective parameter values (red curve) and mean parameter value (blue curves) against results from Monte Carlo simulations (symbols) with two different domain sizes.

variability in the results using the 50 m × 50 m domain because, for a fixed correlation length, the simulated heterogeneities span a larger fraction of the flow field and so less spatially averaging of the effects of these heterogeneities can take place. This result is consistent with Lu et al. (2011, unpublished data), who studied the scale dependence of effective transport parameters and their associated uncertainty and concluded that effective parameters derived at a smaller scale will have a larger uncertainty.

Verification

To test the applicability of the derived effective parameters to field-scale applications, several numerical simulations were conducted for a two-dimensional cross-section of 400 m × 200 m, which was uniformly discretized into a grid size of 2 m × 1 m. The flux boundary was specified at the top with an infiltration rate of 5 mm yr^{-1}, which is typical in the area of Nevada where many of the potential applications of this work exist. The lower boundary was the water table, and a no-flow condition was applied at two lateral boundaries.

First, we conducted a series of Monte Carlo simulations by generating aperture fields and spacing fields using statistics of the aperture and spacing given above, and converted these fields to realizations of K_s, α, and n. For each set of K_s, α, and n realizations, the unsaturated flow equation was solved under the given boundary conditions until steady state was achieved. The statistics of the pressure head field and saturation field were computed from all Monte Carlo simulations. These results were considered as "true" solutions for unsaturated flow in the randomly heterogeneous fractured medium. Because of high computational cost

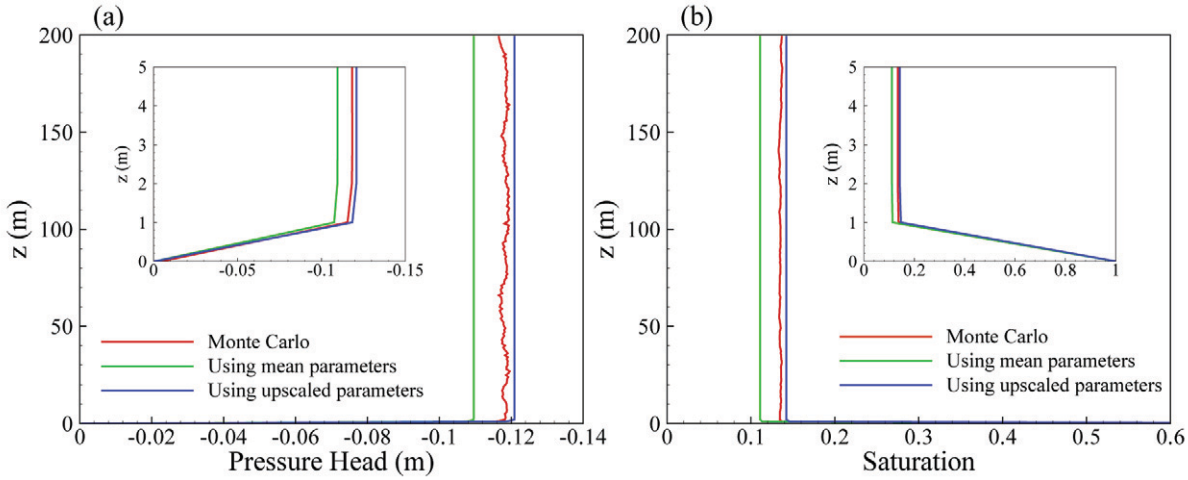

Fig. 6. Comparison of vertical distribution of (a) pressure head and (b) saturation derived from Monte Carlo simulations, a single simulation using the mean parameter values, and a single sim-ulation using the upscaled parameter values.

for each flow simulation, in this study, we conducted 200 Monte Carlo simulations only.

To smooth the mean vertical profile from Monte Carlo results, in additional to averaging over 200 realizations, we also took the average of all vertical columns in the flow domain. This is justified because all nodes at the upper (or lower) boundary have the same infiltration value (or fixed pressure head) and a no-flow condition has been applied to the lateral boundaries. The vertical profile of the true mean solutions was compared with two additional simulations using homogeneous parameter fields as described below. In the second numerical simulation, instead of spatially variable parameters as in the Monte Carlo simulations, the values of parameters K_s, α, and n were taken to be constants computed from the mean aperture and mean spacing. In the third simulation, the parameter values were also constants but using the upscaled effective parameter values.

Figure 6a compares the vertical pressure head derived from three simulations. The inserted plot shows the lower portion of the profile. The figure indicates that the pressure head distribution derived using upscaled effective parameter values is much better (i.e., closer to Monte Carlo results) than that computed from mean parameter values. In fact, the former has a relative error (comparing with MC results) of about 2%, whereas a relative error for the latter is about 10%. Figure 6b shows that saturation estimated with the upscaled parameters agree with the mean saturation of the Monte Carlo results, whereas the saturation estimated from mean parameters calculated from mean aperture and spacing shows larger differences with the Monte Carlo results. Closeness of modeling results using upscaled parameter values to the Monte Carlo results indicates that the upscaling procedure is reasonable and that the effective parameter values derived from this procedure may be used in simulating flow in field-scale problems.

Effective parameter values from our numerical method were derived from the steady state flow condition. However, these effective values are independent of flow state variables (pressure head or saturation) thus can be applicable directly to transient simulations. To verify this, we conducted a set of transient simulations with a similar flow domain setup as in the previous example, except that the initial saturation in the domain was set to 0.2. The comparison of vertical saturation profile (along the middle of the domain) derived from 200 Monte Carlo simulations, a single simulation using the mean parameter values, and a single simulation using the upscaled parameter values at $t = 10^2$ d and 10^5 d are illustrated in Fig. 7. The results from MC simulations are not smooth because they are calculated from the central vertical profile, not averaged over all vertical profiles in the domain. However, the general trend can be clearly seen from the figure. The figure indicates that the results from the simulation with upscaled parameters are much

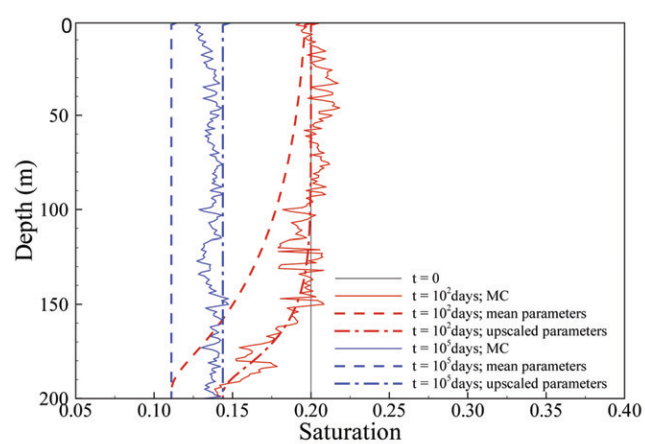

Fig. 7. Comparison of vertical saturation profiles (along the middle of the domain) derived from Monte Carlo simulations, a single simulation using the mean parameter values, and a single simulation using the upscaled parameter values, at $t = 10^2$ d and 10^5 d.

closer to MC results, which means that these effective values can be applicable directly to transient simulations.

Discussion and Conclusions

In this study, we proposed a numerical upscaling procedure for estimating effective parameters of unsaturated, fractured rock that can be applied in larger-scale models over a range of pressure heads and infiltration rates. We accomplished this by creating a numerical permeameter in which the fractured part of the model domain was treated as a stochastic continuum in which saturated and unsaturated hydraulic properties at the local support scale were estimated from stochastically generated distributions of fracture aperture and spacing, a variation of the cubic law, and pore-scale simulations of single, variable-aperture fractures. Vertical correlation lengths for fracture aperture and spacing were estimated from borehole data collected from tuffs in the vicinity of the Nevada Test Site. The permeability and van Genuchten parameters were converted from fracture spacing and aperture using a set of empirical relationships. Simulation results relating effective hydraulic conductivity, mean fracture pressure head and mean fracture saturation were generated for multiple Monte Carlo realizations of the aperture and spacing fields over a range of fluxes in a gravity-dominated flow system at a scale relevant to field-scale applications. This is accomplished by running a number of Monte Carlo simulations at different saturation under a gravity-dominated condition in a domain at the size of grid blocks typical in field-scale simulations, using realizations of K_s, α, and n, . The effective unsaturated conductivity of the entire rock domain for each simulation is determined from the steady state flux at the bottom of the domain. The relationship between the effective unsaturated conductivity and mean pressure head (or saturation) is then fitted with the van Genuchten model to obtain $K_{s,\mathrm{eff}}$, α_{eff}, and n_{eff} for the fractured rock mass. These effective parameters are independent of pressure head or saturation and therefore may be used in field-scale applications. Although these effective parameter values were derived from the steady state flow condition, however, they are independent of flow state variables, and thus can be applicable directly to transient simulations.

The performance of the numerical upscaling procedure was evaluated by comparing the effective unsaturated hydraulic conductivity derived from (i) the mean values of K_s, α, and n, (ii) upscaled effective parameter values $K_{s,\mathrm{eff}}$, α_{eff}, and n_{eff}, and (iii) Monte Carlo simulations; the latter were considered as "true" solutions. The comparison indicates that the upscaled effective parameters outperform (i.e., closer to results from Monte Carlo simulations) the mean parameter values. However, the values of K_s, α, and n estimated from the mean aperture and fracture spacing provide an approximate fit to the detailed Monte Carlo results that may be adequate for modeling flow in many applications.

The numerical simulations presented in this paper merge established concepts that treat frac-tured rocks as a stochastic continuum with concepts of variably saturated flow in heterogeneous porous media to demonstrate a methodology for upscaling the unsaturated hydraulic properties of fractured rock. This is a natural and logical extension of developments that have taken place in both of these fields over the last 20 yr. To illustrate the methodology, we rely on a set of empirical relationships that relate the unsaturated hydraulic properties of fractures to their physical apertures and fracture spacing, and the statistics of aperture and spacing were estimated from tuffs in the vicinity of the Nevada Test Site.

Acknowledgment

This work was supported by Department of Energy (DOE) through Underground Test Area Projects.

References

Bibby, R. 1981. Mass transport of solutes in dual-porosity media. Water Resour. Res. 17(4):1075–1081. doi:10.1029/WR017i004p01075

Berkowitz, B., J. Bear, and C., Braester. 1988. Continuum models for contaminant transport in fractured porous formation. Water Resour. Res. 24(8):1225–1236. doi:10.1029/WR024i008p01225

Finsterle, S. 2000. Using the continuum approach to model unsaturated flow in fractured rock. Water Resour. Res. 36:2055–2066. doi:10.1029/2000WR900122

Khaleel, R., T.-C. J. Yeh, and Z. Lu. 2002. Upscaled flow and transport properties for heteroge-neous unsaturated media. Water Resour. Res. 38:1053–1064. doi:10.1029/2000WR000072

Kwicklis, E. M., and R. W. Healy. 1993. Numerical investigation of steady liquid water flow in a variably saturated fracture network. Water Resour. Res. 29:4091–4102. doi:10.1029/93WR02348

Kwicklis, E.M., F. Thamir, R.W. Healy, and D. Hampson. 1998. Numerical simulation of air- and water-flow experiments in a block of variably saturated, fractured tuff from Yucca Mountain, Nevada. USGS Water-Resour. Invest. Rep. 97-4274.

LeCain, G.D. 1997. Air-injection testing in vertical boreholes in welded and nonwelded tuff, Yucca Mountain, Nevada. USGS Water Resour. Invest. Rep. 96-4262.

Mantoglou, A., and L. W. Gelhar. 1987. Effective hydraulic conductivities of transient unsatu-rated flow in stratified soils. Water Resour. Res. 23:57–67. doi:10.1029/WR023i001p00057

Mualem, Y. 1976. A new model for predicting the hydraulic conductivity of unsaturated porous media, Water Resour. Res. 12:513–522. doi:10.1029/WR012i003p00513

Neuman, S.P. 1987. Stochastic continuum representation of fracture rock permeability as an al-ternative to the REV and fracture network concepts. In: Framer et al., editors, 28th U.S. Symposium on Rock Mechanics, Balkema, Rotterdam, The Netherlands, p. 533–561.

Prothro, L.B. 2008. Analysis of fractures in cores from the tuff confining unit beneath Yucca Flat, Nevada Test Site. Natl. Sec. Tech. Rep. DOE/NV/25946–351.

Tsang, Y.W. 1992. Usage of "equivalent apertures" for rock fractures as derived from hydraulic and tracer tests. Water Resour. Res. 28:1451–1455. doi:10.1029/92WR00361

Tsang, Y.W., C. F. Tsang, F. V. Hale, and B. Dverstorp, 1996. Tracer transport in a stochastic continuum model of fractured media. Water Resour. Res. 32(10):3077–3092. doi:10.1029/96WR01397

van Genuchten, M.Th. 1980. A closed-form solution for predicting the conductivity of unsaturat-ed soils. Soil Sci. Soc. Am. J., 44:892–898. doi:10.2136/sssaj1980.03615995004400050002x

Wildenschild, D., and K.H. Jensen. 1999a. Numerical modeling of observed effective flow be-havior in unsaturated heterogeneous sands. Water Resour. Res. 35:29–42. doi:10.1029/98WR01959

Wildenschild, D., and K. H. Jensen. 1999b. Laboratory investigations of effective flow behavior in unsaturated heterogeneous sands, Water Resour. Res. 35:17–29. doi:10.1029/98WR01958

Wu, Y.S., C. Haukwa and G.S. Bodvarsson. 1999. A site-scale model for fluid and heat flow in the unsaturated zone of Yucca Mountain, Nevada, J. Contam. Hydr. 38:185–215. doi:10.1016/S0169-7722(99)00014-5

Yeh, T.-C. J., L. W. Gelhar, and A. L. Gutjahr. 1985. Stochastic analysis of unsaturated flow in heterogeneous soils, 2, Statistically isotropic media. Water Resour. Res. 21:447–456. doi:10.1029/WR021i004p00447

Zhang, D., and Z. Lu. 2004. An efficient, higher-order perturbation approach for flow in randomly heterogeneous porous media via Karhunen-Loeve decomposition. J. Comput. Phys. 194:773–794. doi:10.1016/j.jcp.2003.09.015

Zheng, Q., S.E. Dickson, and Y. Guo. 2008. On the appropriate "equivalent aperture" for the description of solute transport in single fractures: Laboratory-scale experiments. Water Resour. Res. 44:W04502. doi:10.1029/2007WR005970.

Zhu, J., and D. Sun. 2009. Effective soil hydraulic parameters for transient flows in heterogene-ous soils. Vadose Zone J. 8:301–309. doi:10.2136/vzj2008.0004

Zyvoloski, G.A., B.A. Robinson, Z.V. Dash, and L.L. Trease. 1997. Summary of the models and methods for the FEHM application—A Finite-Element Heat- and Mass-Transfer code, LA-13307-MS. Los Alamos National Lab., Los Alamos, NM.